Development of electrochemical biosensor for direct histamine detection by using selective peptides as biorecognition element

Veronika Vanova[1], Vedran Milosavljevic[1,2], David Hynek[1,2], Lukas Richtera[1,2], Vojtech Adam[1,2]
[1]Department of Chemistry and Biochemistry
Mendel University in Brno
Zemedelska 1, 613 00 Brno
[2]Central European Institute of Technology
Brno University of Technology
Purkynova 123, 612 00 Brno
CZECH REPUBLIC

veronika.vanova@mendelu.cz

Abstract: The level of histamine (HIS) in different food sources is critical as an indicator of food quality and safety. In this context, the proper monitoring of HIS in food is necessary. Electrochemical biosensors, with the possibility of fast, sensitive, and portable technology, represent a new promising approach for direct detection of HIS. Moreover, peptides as biorecognition elements are promising due to their unique properties such as good stability, specific and selective binding to various biomolecules. In this study, the fabrication and optimization of an electrochemical biosensor for direct detection of HIS based-on peptides as recognition elements, is presented. The specific HIS binding peptides (HBP) were immobilized via a sulphonamide bond on 1-amino-2-naphthol-4-sulfonic acid (ANSA), which was electrodeposited on a glassy carbon electrode (GCE). Furthermore, the optimization of the surface coverage with the peptide probe as well as the effect of the pH conditions for HIS binding was investigated. The measured concentrations were from 10 nM (10^{-8} M) to 1 mM (10^{-3} M) and LOD was calculated as 6.53 nM and LOQ as 21.75 mM.

Key Words: histamine, peptide, biorecognition element, electrochemical biosensor, electrochemistry

INTRODUCTION

Histamine (HIS), with its heterocyclic amine structure, belongs to a group of alkaloids that are responsible for various physiological effects in the human organisms. HIS is synthesized from L-histidine by L-histidine decarboxylase and then stored in the granules of mast cells and basophils, the main sources of HIS in the human body (Tanaka et al. 2004). Moreover, HIS plays key roles as a neurotransmitter, hormone mediator, and is involved in the inflammation process and immunity system (Nieto-Alamilla et al. 2016). HIS is essential in human metabolism, but on the other hand, it can be harmful to the organism if it occurs in food at higher levels (Rocha et al. 2016). The digestion of HIS in the human body is mainly secured by enzymes diamine oxidase (DAO). The activity of these enzymes greatly affects the toxic effect of HIS. However, in higher concentrations of HIS in food, the enzymatic system might not be able to eliminate all intake of HIS, and then the poisoning of the organism can occur. HIS is produced as a result of the metabolic activity of microorganisms in food and beverages (Taylor and Eitenmiller 1986). Therefore, HIS can be found mainly in foodstuffs that are rich in proteins, such as fish and meat, as well as in food produced by the fermentation processes such as wine and beer. If there is a higher level of HIS intake in the body, it can be toxic for the organism. Thus, the determination of HIS is an important indicator of freshness or spoilage of food as well as a quality indicator (Papageorgiou et al. 2018).

Comparing with the traditional approaches for HIS detection such as HPLC and ELISA (Önal 2007), several new alternative approaches are currently being investigated (Horemans et al. 2010, Jiang et al. 2015). One of such approaches uses electrochemical biosensors for direct HIS detection (Butwong et al. 2019) with the advantages of quicker, portable technology and high sensitivity benefit.

In this study, a novel electrochemical biosensor for HIS detection is described, which is using short synthetic peptides as biorecognition elements. The specific amino acid sequence, various binding groups, and flexible conformation structure create the unique abilities of peptides such as high specificity and selectivity to the target molecule. Furthermore, they are well known because of their high stability and good catalytic activity with multiple binding groups (Karimzadeh et al. 2018).

Thus, in this study, the peptide with sequence selective for HIS binding was used as a biorecognition layer. For peptide probe immobilization, electropolymerization of the ANSA layer was done. ANSA is characteristic of the possibility of binding with the –NH group via a sulphonamide coupling reaction (Hermanson 2013). HIS selectively binds to the HIS binding peptide (HBP) via hydrogen and ion-strength interaction which are strongly dependent on pH condition. Therefore, this work will mainly focus on the modification and optimization of the biosensor.

MATERIAL AND METHODS

Reagents

Electrodes polishing was provided by Water Based Diamond suspension (0.50 µm) and Alumina Slurries (0.05 µm; 0.30 µm; 1.00 µm) purchased from Electron Microscopy Science, Hatfield, United Kingdom. For electrodes washing ethanol absolute, acetone (≥99.5%) (VWR chemicals, Randor, Pennsylvania, USA) and MilliQ water, 18.20 MΩ/cm, were used.

The other chemicals used in this study were purchased from Sigma-Aldrich (St. Louis, MO, USA) if it is not stated otherwise. 10 mM 1-amino-2-naphthol-4-sulfonic acid (ANSA) was diluted in Phosphate buffered saline (PBS) (pH 7, 25 mM) (Table 1.). 40 mM phosphorus pentachloride (PCl_5) was dissolved in acetone.

HBP probe with sequence CSLESLESLESLE was synthetized by Fmoc solid phase synthesis, closely described at (Mazumdar et al. 2020), by using Liberty Blue peptide synthesizer (CEM, Matthews, NC, USA).

Table 1 Buffers composition

Buffer	Compounds
Phosphate buffered saline	20.00 g NaCl, 0.5 g KCl, 3.6 g Na_2HPO_4, 0.6 g KH_2PO_4 were diluted into 1000 ml of MilliQ water.
Britton-Robinson buffer (B-R)	For B-R at pH 1.81: 1.15 ml of acetic acid, 1.36 ml of H_3PO_4 and 1.24 g of boric acid was added into 500 ml of MilliQ water. For B-R at pH 4: 2.6 ml of 0.2 M NaOH was added into 10 ml of B-R pH 1.81 stock solution. For B-R at 6 pH 4.5 ml of NaOH was added into 10 ml of B-R pH 1.81 stock solution. For B-R at 7 pH 5.4 ml of NaOH was added into 10 ml of B-R pH 1.81 stock solution. For B-R at 8 pH 6.2 ml of NaOH was added into 10 ml of B-R pH 1.81 stock solution (Reynolds III et al. 2013).
Measuring electrolyte solution	5 mM Potassium hexacyanoferrate(II) trihydrate $K_4[Fe(CN)_6]$ and 5 mM Potassium hexacyanoferrate(III) $K_3[Fe(CN)_6]$ in 0.1 M KCl.

Biosensor preparation

The GCE was mechanically cleaned stepwise with 1.00 µm, 0.30 µm, 0.05 µm alumina slurry, and diamond suspension each for 90 s. Between each step, the residual powder was removed by electrodes sonication in acetone, ethanol, and MilliQ water for 3 min in each. Subsequently, the electrochemical cleaning was followed. The three electrodes (working, counter, and reference) were immersed in 0.5 M H_2SO_4 and the CV carrying out potential cycles between −1.2 and +1.2 V and a scan rate of 50 mV/s until the characteristic voltammogram of clean GCE was obtained. After that, working electrodes were washed with MilliQ and dried under argon gas.

The electrodeposition of ANSA was done by immersing electrodes in 4 ml of the solution of ANSA in PBS. The deposition was carried out by CV with a potential set up between +1.5 and −0.5 V and with scan rate 20 mV/s. The deposition was running eight cycles until the steady CV voltammogram was formed. In the following step, the exchange of the sulfonic group from ANSA into the sulfonyl group was done by incubation of 40 mM PCl_5 in acetone for 30 min (Wang et al. 2013). After obtaining the sulfonylated ANSA the peptide probe was applied on the electrode surface by dropping 10 µl of peptide probe (50 µM) diluted in MilliQ and then dried at 40 °C for 40 min. Before measuring the biosensor with peptide, the probe was washed with PBS and MilliQ water in each for 1 min.

HIS binding was carried out in B-R buffer in various pH ranges. HIS at exact concentration was diluted in B-R and subsequently incubated with peptide attached to the electrode for 1 hour. After that, the electrode was slightly washed and measured by Electrical impedance spectroscopy (EIS), Square wave voltammetry (SWV), and Cyclic voltammetry (CV).

Electrochemical measurement

All electrochemical measurements were performed by Autolab PGSTAT302N and processed with NOVA 2.1.4 software (Metrohm, Herisau, Switzerland). Three electrode connection was used for each electrochemical measurement, where GCE electrode act as working electrode (BASI, West Lafayette, USA), platinum wire as the counter electrode and 3 M Ag/AgCl as the reference electrode (Metrohm, Herisau, Switzerland). All electrochemical measurements were undertaken in measuring electrolyte solution (Table 1).

SWV experiments were performed at potential starting from −0.5 V and ending at +1.0 V, step potential was set up at 0.001 V, modulation amplitude at 0.02 V and Frequency 25 Hz. CV was running in the potential scan range +0.6 V and +0.2 V and scan rate 50 mV/s. EIS was conducted using open circuit potential, frequencies in range of 0.01 Hz to 10 kHz, DC potential was set at 0.23 V and amplitude of 5 mV.

RESULTS AND DISCUSSION

Modification of the electrode

The monitoring of step-by-step electrode modification was recorded by CV measurement. For each modification step, a characteristic voltammogram was obtained (Figure 1). The yellow curve corresponds to the bare electrode where a pair of typical redox peaks for GCE occurred. The peaks are corresponding to the electrochemical process of electron exchange of $[Fe(CN)_6]^{3-/4-}$ redox couple.

In the first step of electrode modification, the electropolymerization of ANSA was done by CV (Figure 1; red curve). It is clear that the redox peaks visibly decreased, with a layer of ANSA on the electrode surface, which can be explained by the fact, that electron transfer of $[Fe(CN)_6]^{3-/4-}$ was blocked by the ANSA. There are two possible reasons of why a blockage of electron transfer occurs. One is that ANSA is a physical barrier for electron transfer between electrode and electrolyte and the second can be due to electrostatic repulsion (Tabanlıgil Calam and Yılmaz 2020).

Figure 1 CV voltammograms of each step of the GCE modification

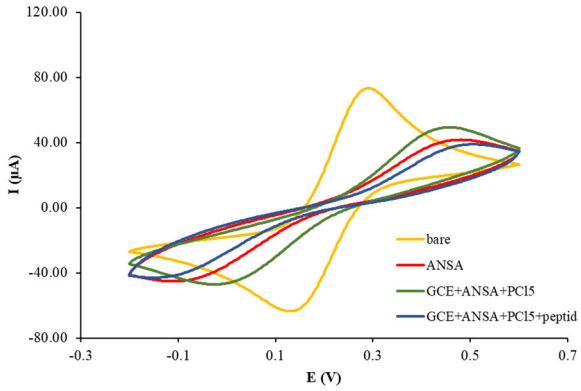

For conjugation of the peptide with sulfonic acid, the sulfonyl chloride derivate pre-step must be done. The derivate is prepared by reaction of the sulfonic acid with PCl_5 in acetone solution (Figure 2)

(Hermanson, 2013). In this step, transfer of sulfonic group from ANSA into the sulfonyl group reaction was done by the incubation of electrode with PCl_5, the redox peaks of CV appreciably increased (Figure 1; green curve). Explanation of this can be that sulphuric acid groups were negatively charged and after binding with Cl, it turns into a neutral sulfonyl group, which allows better diffusion of electrons to the electrode surface (Wang et al. 2013).

Therefore, a sulfonated electrode was coupled with a peptide probe by dropping 10 µl of peptide (50 µM) and dried in an oven at 40 °C for 40 min. In this modification step, the height of the redox peaks decreased dramatically because the peptide does not have a conductive character, thus it is blocking charge transfer between electrode and electrolyte.

Optimization of peptide probe coverage

For obtaining the best sensitivity of the biosensor, the electrode surface coverage with the peptide probe must be optimized. The higher surface loading density of a biorecognition element was desired to maximize the number of available analyte binding sites. For this reason, it is necessary to cover all binding sites of the ANSA with a peptide probe to achieve higher density surface coverage. However, steric hindrance must be taken under the account as well. In this study, different concentrations of the peptide probe were applied on the electrode surface to investigate how much peptide can be caught on the electrode surface. Various concentrations (10.0 µM, 25.0 µM, 50.0 µM, 100.0 µM; 500.0 µM) of the HBP were applied on the GCE modified with ANSA and PCl_5. The peptide probe was dropped on the modified electrode at exact concentration and subsequently dried in oven for 40 min at 40 °C. After the washing step the measurement by EIS was following (Figure 2).

The results show that the best electrode surface coverage was obtained at 50 µM concentration of the HBP, which was assumed according the largest Nyquist semicircle, which indicate the lowest charge transfer resistance. Peptides are usually not electrochemically active, thus they act more as an isolator, which means the more peptide is on the electrode the larger diameter of Nyquist semicircle will occur. The lowest concentrations of the peptide (10 µM and 25 µM) had clearly smaller diameter of semicircle, which indicate the not fully covered electrode surface. On the other hand, in the higher concentrations of peptide, decreasing of semicircle diameter was occurred as well. It happened possibly because of saturated electrode surface.

Figure 2 Influence of the various peptide concentrations on EIS records. A – Nyquist plots from measurement of various peptide concentrations. B – dependence of peptide probe concentrations on the diameter of the semicircle. The error bars are represented by standard 5% error of measurements (n=3).

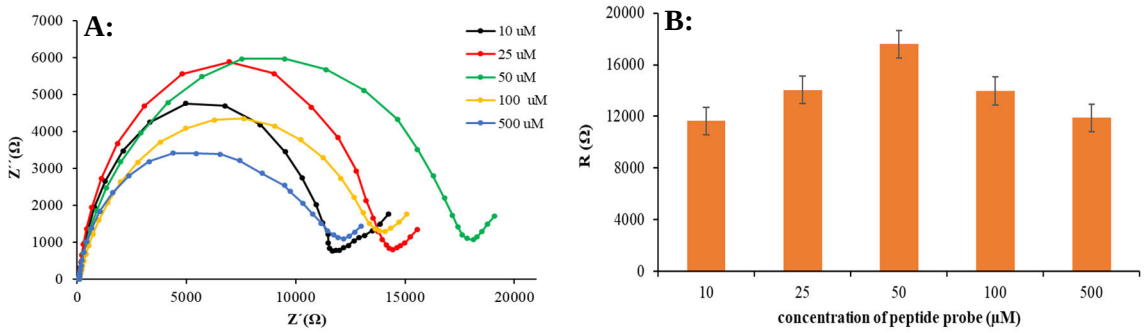

Histamine binding buffer optimization

In this section, the optimization of different binding buffers for HIS is discussed. Because different pH values of peptide and HIS indicate the protonated and deprotonated state of these molecules, various pH conditions were tested. HIS is mainly presented in the single protonated state which corresponds to 6.9 to 10.4 pH range (Jiang et al. 2015). Moreover, HBP is also affected by different pH conditions where its protonated state is ranging at pH 6.0 to 7.0. Peptide-HIS binding is presented based on specific hydrogen and ion-dipole interaction. Therefore, this formation is strongly dependent on the optimal pH condition.

Here we report the measurement focusing on optimization of the right condition for peptide-HIS binding in different buffers. The peptide-modified electrode was incubated in 1 mM solution of HIS in B-R buffer at pH 4; 6; 7; 8 and MilliQ water. The results show the best binding efficiency by using

B-R pH 7, which was observed by EIS measurement (Figure 3). At pH 6–7, the Nyquist semicircle is the smallest, which indicates the higher charge transfer resistance. The more HIS is caught on the electrode surface the higher charge transfer will occur. At this condition, HIS is in the single protonated state and shows the best binding response with HBP, which is also in a protonated state. The good results were also presented in MilliQ water, which represents conditions between pH 6–7. However, the stability of the peptide-HIS linkage was unstable.

In acidic conditions, HIS is almost fully protonated, while peptide is deprotonated in acidic pH. For this reason, only a weak hydrogen bond can occur between peptide and HIS. This statement was verified by EIS measurement at B-R pH 4 (Figure 3), where the charge transfer resistance is the lowest, thus the diameter of the Nyquist semicircle is the highest, which is caused by only a small amount of HIS bonded to the peptide.

At alkaline pH, HIS starts to a deprotonated, and only a small amount of hydrogen bonding can be originated, which is visible on the increasing diameter of the Nyquist plot in Figure 3A.

Figure 3 Optimization of pH conditions for HIS binding. A – EIS records of 1 mM HIS in different pH buffers. B – dependence of pH conditions on the diameter of the semicircle. The error bars are represented by standard 5% error of measurements (n=6).

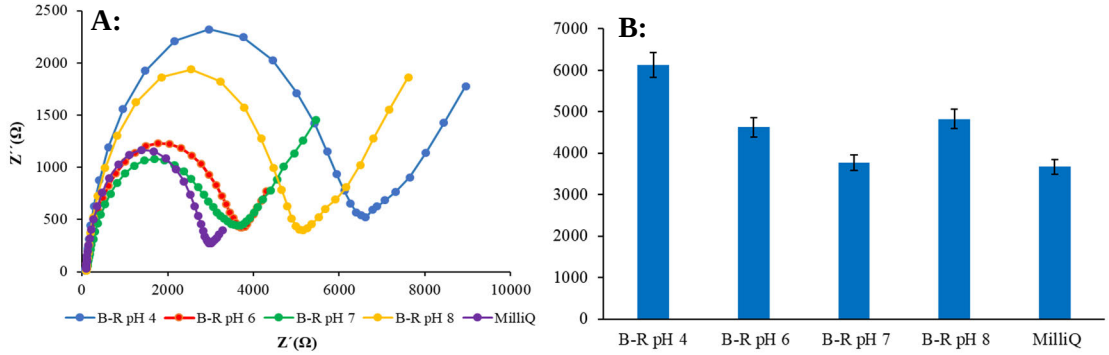

Calibration curve

Biosensor ability for HIS detection was measured in different concentrations by SWV (Figure 4). This study was aimed to investigate if the charge transfer is increasing with an increasing amount of the HIS. Concentrations of HIS are reported as log *c* (M) for displaying their linear dependence. Calibration curve (Figure 4) presents the concentration from 10 nM (10^{-8} M) to 1 mM (10^{-3} M). LOD and LOQ values were counting true the regression equation. The LOD was calculated as 6.53 nM and the LOQ as 21.75 nM (Table 2). The results show that the biosensor is sensitive enough for HIS values, which are ranging in food from µM to mM concentrations. (Wang at al. 2013).

Figure 4 Calibration curve for HIS detection.

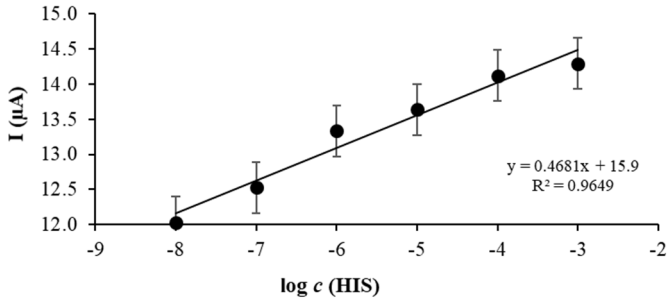

Table 2 Analytical table

Sample	Regression Equation	Linear dynamic range log *c* (M)	R^2	LOD (nM)	LOQ (nM)	RSD (%)
histamine	y = 0.4681x + 15.9	–8 to – 3	0.9649	6.53	21.75	10.80

CONCLUSION

To summarize the issue up, the electrochemical biosensor with HBP as a recognition element for direct HIS detection was designed. In this study, the step-by-step modification and optimization of the biosensor are presented. Moreover, it was demonstrated that a wide range of HIS concentrations is possible to detect with the suggested biosensor. Thus, the biosensor is prepared for the next experiments and testing with real samples, such as wine or other fermented beverages.

ACKNOWLEDGEMENTS

The research was financially supported by the IGA MENDELU AF-IGA2020- IP009.

REFERENCES

Butwong, N. et al. 2019. Electrochemical sensing of histamine using a glassy carbon electrode modified with multiwalled carbon nanotubes decorated with Ag-Ag_2O nanoparticles. Microchimica Acta, 186(11): 714.

Hermanson, G.T. 2013. The reactions of bioconjugation. In Bioconjugate techniques. Elsevier, pp. 229–258.

Horemans, F. et al. 2010. MIP-based sensor platforms for the detection of histamine in the nano- and micromolar range in aqueous media. Sensors and Actuators B: Chemical, 148(2): 392–398.

Jiang, S. et al. 2015. Surface plasmon resonance sensor based on molecularly imprinted polymer film for detection of histamine. Sensors and Actuators B: Chemical, 221(1): 15–21.

Karimzadeh, A. et al 2018. Peptide based biosensors. TrAC Trends in Analytical Chemistry, 107(1): 1–20.

Mazumdar, A. et al. 2020. Peptide-Carbon Quantum Dots conjugate, Derived from Human Retinoic Acid Receptor Responder Protein 2, against Antibiotic-Resistant Gram Positive and Gram Negative Pathogenic Bacteria. Nanomaterials, 10(2): 325.

Nieto-Alamilla, G. et al. 2016. The histamine H3 receptor: structure, pharmacology, and function. Molecular Pharmacology, 90(5): 649–673.

Önal, A. 2007. A review: Current analytical methods for the determination of biogenic amines in foods. Food Chemistry, 103(4): 1475–1486.

Papageorgiou, M. et al. 2018. Literature update of analytical methods for biogenic amines determination in food and beverages. TrAC Trends in Analytical Chemistry, 98: 128–142.

Reynolds III, J.E. et al. 2013. Spectral and redox properties of the GFP synthetic chromophores as a function of pH in buffered media. Chemical Communications, 49(71): 7788–7790.

Rocha, S.M. et al. 2016. Histamine induces microglia activation and dopaminergic neuronal toxicity via H1 receptor activation. Journal of Neuroinflammation, 13(1): 1–16.

Tabanlıgil Calam, T., Yılmaz, E.B. 2020. Electrochemical determination of 8-hydroxyquinoline in a cosmetic product on a glassy carbon electrode modified with 1-amino-2-naphthol-4-sulphonic acid. Instrumentation Science & Technology, 1–20.

Tanaka, S. et al. 2004. Expression of L-histidine decarboxylase in granules of elicited mouse polymorphonuclear leukocytes. European Journal of Immunology, 34(5): 1472–1482.

Taylor, S. L., Eitenmiller, R. R. 1986. Histamine food poisoning: toxicology and clinical aspects. CRC Critical Reviews in Toxicology, 17(2): 91–128.

Wang, Q., et al. 2013. A sensitive DNA biosensor based on a facile sulfamide coupling reaction for capture probe immobilization. Analytica Chimica Acta, 788(1): 158–164.